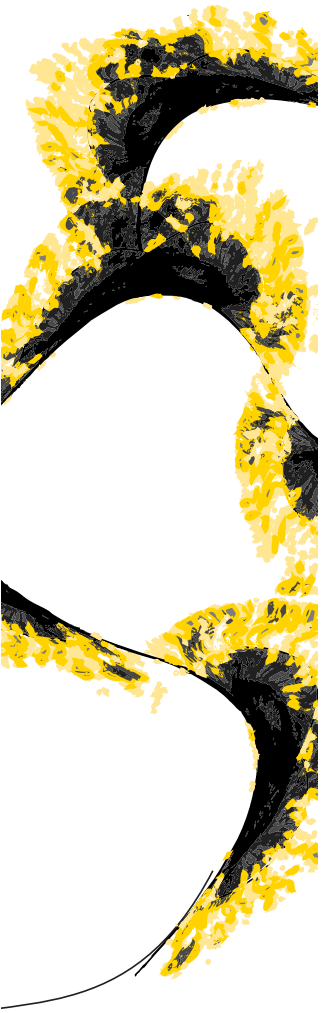

RAM ROBOTICS AND MECHATRONICS

THE ACCURACY OF A FEM MODEL IN PREDICTING PHANTOM DEFORMATION

H.J.L. (Louise) Schneider

MSC ASSIGNMENT

Committee:
prof. dr. ir. L. Abelmann
dr. V. Groenhuis, MSc
dr. F.J. Siepel, MSc
dr. ir. L.J. Spreeuwers

March, 2021

014RaM2021
Robotics and Mechatronics
EEMCS
University of Twente
P.O. Box 217
7500 AE Enschede
The Netherlands

UNIVERSITY OF TWENTE. | TECHMED CENTRE UNIVERSITY OF TWENTE. | DIGITAL SOCIETY INSTITUTE

Abstract

Purpose Previous research has resulted in a FEM model of a breast phantom, however it has not been examined yet if this model is accurate enough to predict the position of a tumor. If the FEM model is accurate and predicts the position of the tumor when the breast is deformed by an ultrasound probe than this FEM model can be be part of the solution in combining ultrasound and MRI data.

Methods In this model two types of real models are used, a breast phantom and gelatin cuboids. There is also a FEM model of the breast phantom and a FEM model of the gelatin cuboid with size 7x5x5 cm. The gelatin models are deformed with gravity and this deformation is compared to the corresponding FEM model. The breast phantom is deformed with gravity and an ultrasound probe and this deformation is also compared to the corresponding FEM model. The error of the stereo camera is measured by measuring distances on a checkerboard.

Conclusions The FEM model predicts the deformation of the breast phantom accurate enough to find the position of a tumor with pT stage 2 or larger. The random error of the stereo camera is so large that it is difficult to find the breast phantom elasticity, there is a wide range of possible values. Researchers that want to predict the position of a smaller tumor can examine this FEM model with a better measuring system. The error of the stereo camera was a limiting factor in examining the FEM model.

Contents

Chapter 1

Introduction

The chance of a woman in the Netherlands to get breast cancer is 1 out of 7 [1], making this the most common type of cancer women may suffer from. Extensive programs are in place to detect breast cancer in an early phase and start treatment as soon as possible to minimize morbidity and the treatment impact [2]. To diagnose breast cancer, biopsies are to be made to determine if the irregularities detected are indeed cancer induced and to determine the type of cancer. Using MRI scans detected tumors can be as small as 5 millimeters [3]. Taking biopsies from tumors of small sizes requires high precision positioning of a needle. The research of the MURAB project [2], MRI and Ultrasound Robotic Assisted Biopsy, can improve the precision of positioning a needle in biopsies and this can improve the diagnostic techniques of breast cancer.

A mathematical model has been developed to predict the deformation of breast tissue and the position of lesions. When an ultrasound probe is moving over the breast and when a needle is inserted in the breast tissue these deformations occur. This mathematical model needs to be verified to find out if the position of the lesion is predicted accurately enough. This research is part of the MURAB [2] project which aims to improve the diagnosis of breast cancer.

The MURAB project [2] has the ambition to improve both the precision and effectiveness of breast biopsy. By using ultrasound in addition to MRI the amount of time spent on MRI is reduced which reduces the costs compared to only using MRI. Breast cancer is a common type of cancer and a tool like MURAB can improve cancer diagnosis without being too expensive.

The model that is evaluated in this research is an important tool to find the position of the lesion. First the high precision MRI scan is used to find the position of the lesions. Then the breast deformation model is used to predict the position of the lesion when the breast is deformed by the ultrasound probe and when a needle is inserted into the breast. The patient is in prone position during MRI, ultrasound, and biopsy [4]. To summarize this process MRI is used to find the position of the lesion and after that ultrasound in combination with the breast deformation model is used to find the lesion again for the biopsy. This breast deformation model is the result of prior research.

To evaluate the model's applicability, it is this project's goal to design and execute experiments to assess the model's predictive accuracy by comparing the deformation of a breast phantom to the model's predicted deformation. The performance of the model will be assessed by testing if the predicted position of the lesion is sufficient to do a biopsy of the breast lesion.

1.1 State of the art

In earlier studies of the MURAB project [2] an analytical method has been developed which can compute the elasticity of breast phantoms from a set of MRI scans [4]. In this research four breast phantoms are tested and the analytically derived elasticity differs from the numerical elasticity by 18% on average [4]. In this research is concluded that this error is small enough to get an accurate elasticity of the breast phantom [4].

A real time deformation tracking system for breast biopsy has been developed using stereo camera [5]. In this research this system is successful in tracking two out of three world coordinates. This research can be used as a base for the tracking system.

1.1.1 Mechanical properties of the human breast

It can be challenging to find the mechanical parameters of the human breast. The breast is an organ that consist out of multiple tissues that each have different mechanical properties[6]. Also the ratio between these tissues can differ a lot across a population, which depends on factors such as age, physiological conditions, and pathophysiological state of an individual[6]. In order to create a model of the breast some simplification of the biomechanical behaviour of the breast, as discussed in section 1.1.2, has to be made[6].

The human breast is responsible for lactating. They are tear-shaped glands located on the chest, on the pectoralis major muscle. The internal structures of the breast are contained by the superficial and deep fascia. Within these layers are the secretary glands which produce milk. These glands connect through a network of lactiferous ducts to the nipple. The ducts and glands are surrounded by a combination of fibrous and adipose tissue. The proportion of fibrous and adipose tissue varies between individuals and is dependent on age. Cooper's ligaments provide support to the breast and allow the breast to maintain its shape[7].

In breast cancer therapy breast tumor severity and size is categorized in pT stages [8]. Tumors in pT stage 1 are recognizable on MRI when they are as small as 5 mm [3] while pT stages 2, 3, and 4 indicate minimal size of tumors of 2 cm or more which can be detected using ultrasound [3].

Most researchers assume that the breast is homogeneous and elastic [6]. It is also usually assumed that the breast is incompressible [6]. It is possible to create a heterogeneous model of a human breast, however it is a lot more time consuming to create such a model for every single patient.

From direct communication it became clear that Tagliabue tried to create a heterogeneous model to compare to the homogeneous model. However the heterogeneous model is very complex and the results were unsatisfactory. This shows how difficult such a model is.

As described in [9] a method has been developed to measure the elasticity of the breast using MRI. Two MRI scans are made and the difference is the direction of gravity. In this paper the authors used the knowledge that the deformation of an object in a gravitational field is the result of elongations of tissue, which depends on the local ratio of tensile stress and the Youngs modulus. In this paper they assumed that the tensile stress only depends on the vertical position of the object. By measuring the elongation of the breast they can calculate the Youngs modulus. The deviations between the measured elasticity using this method and simulations using FEBio and SOFA were up to 18%. So this method could be very useful to adapt the breast model to a new patient.

1.1.2 Biomechanical behaviour of the human breast

In previous research [10] different strategies of modelling probe tissue interaction have been compared. Each method has a different compromise between accuracy, speed, and stability. All of the methods were based on a homogeneous model.

A finite element model converts the system of partial differential equation describing Newton's second law into a system of algebraic equations which can be solved numerically[10], so the problem will look like:

$$\mathbf{Ma} = \mathbf{f}(t, \mathbf{v}, \mathbf{a}) \tag{1.1}$$

In which M is mass, t is time, v is velocity, f is force, and a is acceleration. In earlier studies of the deformation of the phantom the FEM model in SOFA and the real model could differ up to 9% for cylindrical shapes, and up to 18% for other shapes that are also supported by a planar base[11].

The method based on Lagrange multipliers (LM) treats contacts as constraints [10]. The equations that result from this are described in research of Tagliabue [10].

The LM approach leads to a stable and robust handling of contacts, however the computation time is quite large. Another advantage of this method is that the contact forces are accurately estimated, which is helpful in robot control loops [10]. The LM approach was also compared to other approaches like penalty method, prescribed displacements method, and position-based dynamics (PBD) method.

1.2 Problem Statement

To evaluate the model's predictive accuracy, experiments have to be designed and executed to test the assumptions made in developing the model. Using a breast phantom, both the deformation at the surface of the breast as well as positions within the breast phantom are to be tracked while applying a simulated deformation by a ultrasound probe or needle, comparing the actual positions of the markers and comparing them to the predicted positions.

The model is considered accurate if it can be used to predict the position of tumors in pT stage 2, 3 and 4, these tumors are at least 2 cm in diameter. It is expected that the model is not accurate enough for pT 1 tumors because of their very small sizes. When the error of the model is 1 cm of more off from the actual position it is possible that the needle will miss the tumor. The aim of this research will be that the error of the SOFA model must be smaller than 0.5 cm. This value is chosen because it is desirable that the error is much smaller than 1 cm to compensate for an unknown error in the needle tip position.

1.3 Research Questions

Primary Research Question Is the FEM model able to predict the deformation of a breast phantom caused by an ultrasound probe and the force of gravity accurately enough to do a biopsy of the tumor?

Is it possible that a FEM model of a breast phantom and gelatine cuboid phantom can predict the deformation caused by gravity or ultrasound probe of the corresponding phantom accurately enough to predict the position of a tumor located in the phantom.

Secondary Research Questions

- What is the error of the used stereo camera?
- How can the Youngs modulus of a gelatin cuboid be determined?
- What is the deformation of two gelatin cuboids when they are stacked on top of each other?
- Is the FEM model able to predict the deformation of a gelatin cuboid using the Youngs modulus?
- How can the Youngs modulus of the phantom be determined?
- What is the maximum error in the derformation of the phantom caused by the probe?

1.3.1 Relevance and importance of the research

In verifying the predictive accuracy of the deformation model in breast phantoms, using the positions of markers at the surface of the phantom, the model's applicability in predicting the phantom deformation can be tested. This research might be repeated in clinical trials on real breast tissue.

Chapter 2

Method

This chapter will explain how the stereo camera is calibrated and how the error is the stereo camera is determined. A lot of experiments are repeated with both a cuboid and a phantom, the reason for this is that a simple analytical model of the deformation of the cuboid under gravity can be created and it is not possible to create such a simple model for the phantom. Simulations of how the cuboid and phantom deform under gravity are done in SOFA, this data is exported to Matlab and the height of the model is measured. The height according to the analytical model is also measured. The heights of the real phantom and the real cuboid are measured using the stereo camera. The deformation of the phantom caused by the probe is also measured using the stereo camera.

2.1 Calculate error of stereo camera

For this experiment the Stereo Camera Calibrator App [12] in Matlab is used. Eight pairs of stereo pictures of a checkerboard are taken and the Stereo Camera Calibrator app calculates the stereo parameters using these pictures, as shown in figure 2.1. The stereo parameters consists out of the camera parameters of both cameras and their geometric relationship[12]. The camera parameters consist of the intrinsic, extrinsic, and lens distortion parameters of a camera[12]. The stereo parameters can be used to calculate the distance of a point to the cameras[12].

To calculate the error of the stereo camera, the checkerboard that is used for calibration is used again, because the checkerboard provides multiple points on one stereo image and the distance between the points is known. The checkerboard pattern and the points on the stereo pictures are detected. The position measured by the stereo camera and the actual position of the points are used to calculate the error of the stereo camera.

To calculate the error four pairs of stereo pictures are created with the checkerboard under the angles 20°, 30°, 40°, and 50°. The pictures are undistorted using the undistortImage function in

Figure 2.1: The detected points on the checkerboard

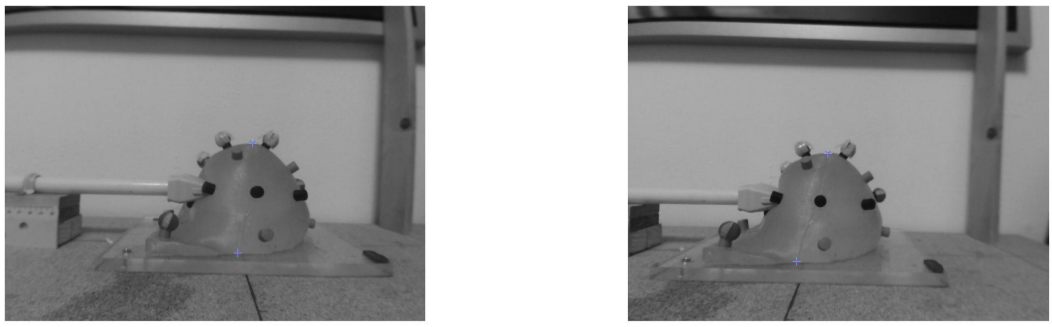

(a) image of camera 1 with points

(b) image of camera 2 with points

Figure 2.2: Images of both cameras with height points

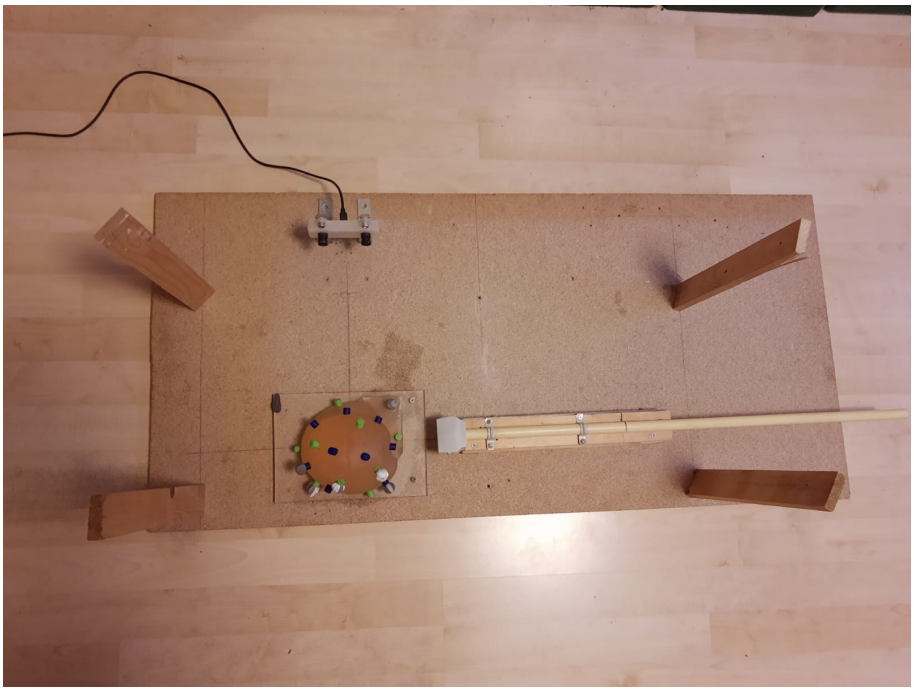

Figure 2.3: The position of the breast phantom relative to the camera

Matlab [12] and next the distances between points in y direction of the checkboard are calculated. The total distance that should be measured between the points is $20mm$.

2.2 Measure height of phantom

The camera is positioned such that the z axis of the coordinate system is along the height of the phantom. The position of the phantom to the camera is shown in figure 2.3.

In figure 2.2 the undistorted images of both cameras with the top and bottom points are shown. The images are undistorted using the undistortImage [12] function in matlab with the camera parameters [12] of the corresponding camera. The three dimensional position of the top and bottom points are calculated using the triangulate function [12] in matlab and the stereo parameters of the stereo camera.

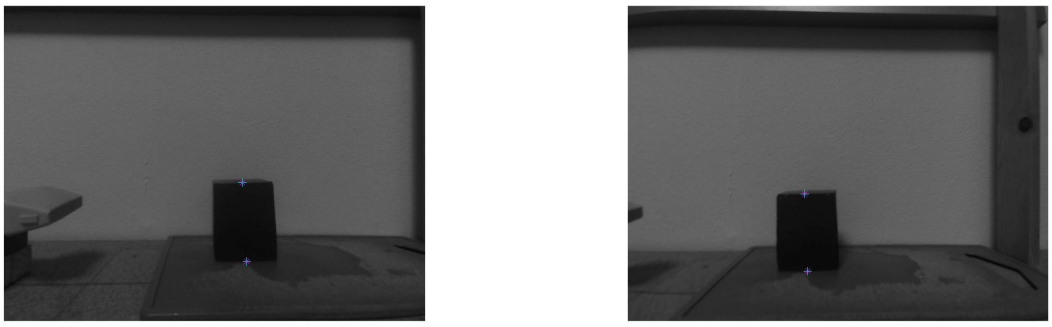

(a) image of camera 1 with points

(b) image of camera 2 with points

Figure 2.4: Images of both cameras with height points

2.3 Measure height of the FEM model in SOFA

The two dimensional datafile in outData, the folder in which SOFA saves the shape and position of the model, is imported in Matlab using the Import Data function. For the delimiter 'tab' is used and the data is stored as a Matlab table. Than the x, y, and z coordinates need to be split, this is done by using the strsplit function in Matlab to split at every space. This is described in algorithm 1. The height of the model is found by calculating the difference between the particle with the highest z value and the particle with the lowest z value.

Algorithm 1 Import SOFA data in Matlab

```
read 'BreastVisu2d_m_allpos_x.txt' as table 'data'
create structure 'dataStruct'
if this is not the first row of 'data' then
    split 'data' at every space
    save split data in 'dataStruct.particleName'
else
    save 'data' in 'dataStruct.time'
```

2.4 Measure height of cuboid

The camera is positioned such that the z axis of the coordinate system is along the height of the phantom.

In figure 2.4 the undistorted images of both cameras with the top and bottom points are shown. The images are undistorted using the undistortImage [12] function in matlab with the camera parameters [12] of the corresponding camera. The three dimensional position of the top and bottom points are calculated using the triangulate function [12] in matlab and the stereo parameters of the stereo camera.

2.5 Compare shape of FEM model and phantom

The two dimensional datafile in outData, the folder in which SOFA saves the shape and position of the model, is imported in Matlab using the Import Data function. For the delimiter 'tab' is used and the data is stored as a Matlab table. Than the x, y, and z coordinates need to be split, this is done by using the strsplit function in Matlab to split at every space.

2.6 Phantom deformation caused by gravity

The mesh that is used in the SOFA model is created using an MRI scan of the phantom. In the MRI the phantom is deformed under gravity, so the mesh that is used in SOFA is already deformed

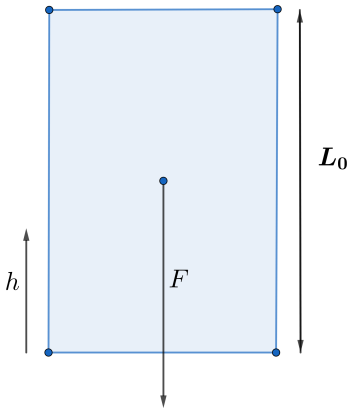

Figure 2.5: The cuboid with variables

by gravity. The goal is to find out if the deformations caused by gravity are calculated properly using SOFA, and this is not directly possible with a mesh that is already deformed.

It the mesh is already deformed under gravity than the initial shape should be found by letting gravity work in the upwards direction. This is however still not comparable with the actual phantom. By letting the gravity work twice in the upwards direction the deformation should be achieved that the phantom has when hanging upside down.

To estimate the Youngs modulus of the phantom multiple simulation are done with different Youngs moduli. The Youngs modulus that predicts the same deformation when the phantom is hanging upside down is the modulus that is used for all SOFA simulations for the phantom.

2.7 Calculating the Youngs modulus of a gelatin cuboid

To study the behaviour of the gelatin cuboid under gravity some assumptions have to be made. The first assumption is that the deformation of the cuboid can be determined by using the mean Youngs modulus of gelatin. The second assumption is that the Youngs modulus of the cuboid is everywhere the same in the cuboid. The third assumption is that the mass density is everywhere the same in the cuboid. The fourth assumption is that the elasticity of the gelatin is linear and that there are no additional terms to the elasticity equations are needed than the Youngs modulus. The fifth assumption is that the deformation of the cuboid is only elastic deformation.

The mass $m(h)$ is the mass that is working on the height h, which is described in figure 2.5, of the cuboid. This mass is the mass of the cuboid from height h to L_0, which is also described in figure 2.5. So the mass that is working on a layer lower in the cuboid is larger than the mass that is working on a layer higher in the cuboid. The mass $m(h)$ on layer h of the cuboid is calculated by integrating the mass density in x and y direction and than the integration for h to L_0 to find the mass on layer h, which can be seen in equation 2.1. The z direction is in the same direction as h, the x direction is from left to right, and the y direction is the depth. The assumption is made that the gelatin has the same mass density in all directions, so the equation can be simplified to an equation dependent on the surface area of a slice at a certain height, that height, and the mass density. The surface area per layer $A(h)$ is actually a constant before deformation of the cuboid.

$$\begin{aligned} m(h) &= \int_h^{L_0} \iint \rho(x,y,z)\,\mathrm{d}x\mathrm{d}y\mathrm{d}z \\ m(h) &= \rho A(h)(L_0 - h) \end{aligned} \tag{2.1}$$

Using this simplification of the mass, the equation of the gravitational force can be derived. From the gravitational force the stress, $\sigma(h)$, and the strain, $\epsilon(h)$, can also be derived, which is shown in equation 2.2. There is the assumption that gelatin is in-compressible so the volume will always be the same, also after deformation. Another assumption in this application is that the Youngs modulus E is constant.

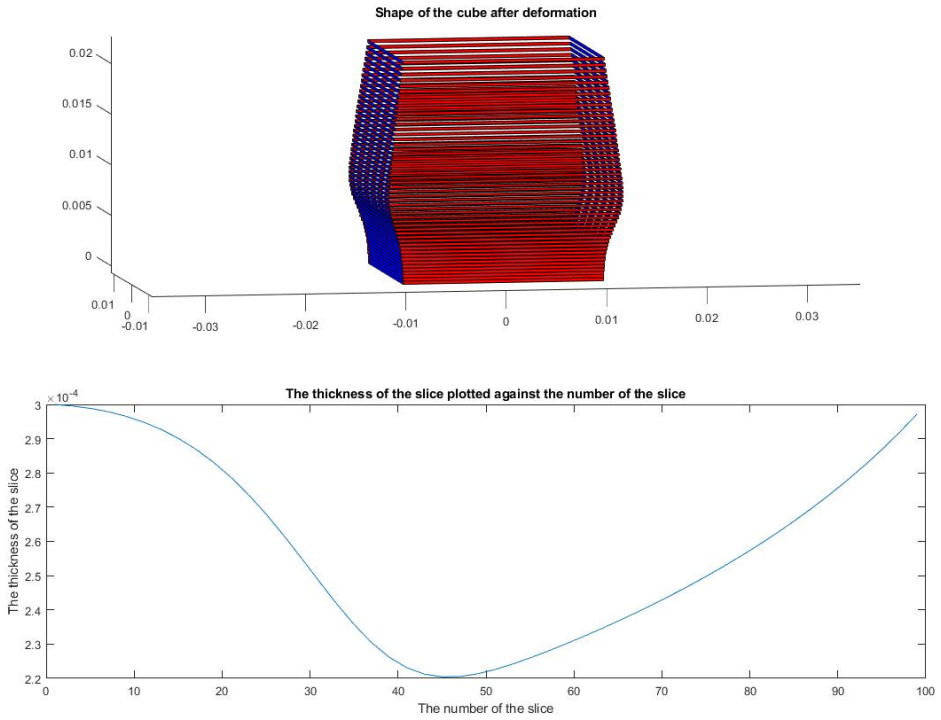

Figure 2.6: The cuboid shape as predicted by Matlab. It can be concluded that the friction with the surface that the cuboid is standing on has influence on the final shape of the cuboid. The surface under the first part of the line is the same as the surface under the second part of the line. That suggest that when the deformed cuboid is cut in half at half of the height the volume of both parts will be the same.

$$\begin{aligned} F(h) &= gm(h) \\ \sigma(h) &= \frac{F(h)}{A(h)} = g\rho(L_0 - h) \\ \epsilon(h) &= \frac{\sigma(h)}{E} = \frac{g\rho(L_0 - h)}{E} \end{aligned} \tag{2.2}$$

In order to find the total deformation, ΔL, of the cuboid the strain from equation 2.2 has to be integrated over the initial length of the cuboid, which is shown in equation 2.3. The deformation ΔL will always be smaller than the initial length L_0, using equation 2.3 the minimal Youngs modulus for the cuboid with an initial height 7.0 cm will be 343 Pa.

$$\begin{aligned} \Delta L &= \frac{g\rho}{E} \int_0^{L_0} (L_0 - h)\, \mathrm{d}h \\ \Delta L &= \frac{g\rho}{E} \frac{L_0^2}{2} \end{aligned} \tag{2.3}$$

The height of the cuboid is measured using a stereo camera. The stereo camera is calibrated as described in section 2.1. The middle top position and middle bottom position is measured using the stereo camera and the measured height is the difference between these points in y direction.

When the deformation is calculated for every layer in the cuboid the shape of the cuboid after deformation can be predicted. This is shown in figure 2.6.

2.7.1 Doubling the height of the cuboid

The initial height of the cuboid is $2L_0$ because the initial height of the first cuboid which was half the height is L_0. The surface area and the Youngs modulus will stay the same. The new equation for the mass is now $m(h) = \rho A(h)(2L_0 - h)$. The gravitational force is still $F(h) = gm(h)$, the stress is still $\sigma(h) = \frac{F(h)}{A(h)}$, and the strain is still $\epsilon(h) = \frac{\sigma(h)}{E(h)}$. So the new strain is $\epsilon(h) = \frac{g\rho(2L_0-h)}{E(h)}$ and to find the deformation this strain is integrated from 0 to $2L_0$, as shown in equation 2.4.

$$\begin{aligned} \Delta L &= \frac{g\rho}{E} \int_0^{2L_0} (2L_0 - h)\,\mathrm{d}h \\ \Delta L &= \frac{g\rho}{E} 2L_0^2 \end{aligned} \tag{2.4}$$

2.7.2 Stacking two cubes on top of each other

When two cubes of the same size and material are stacked on top of each other the gravitational force on the bottom block is twice as large as the gravitational force on the top block. It is expected that the bottom block will deform twice as much in height than the top block according to formula 2.3

Chapter 3

Results

3.1 Stereo camera error

The distance of six checkerboard squares is measured in y direction of the checkerboard, as described in section 2.1. The actual distance, the measured distance, and the absolute error are plotted in figure 3.1. The angle of the checkerboard is the angle the checkerboard makes with the ground. It is observed that the relationship between the angle of the checkerboard and the measured distance can be described with a polynomial with a slope of zero.

The absolute error is also plotted when the actual distance increases in figure 3.2. The distance of the square in y direction of the checkerboard to the distance of seven squares in y direction of the checkerboard is measured, one square is 20 mm long. In figure 3.2 the actual distance, measured distance, and absolute error is plotted against the amount of squares. It is observed that a one dimensional polynomial can describe the relationship between the measured distances and the number of squares and that a one dimensional polynomial can describe the relationship between the absolute error and the number of squares. The polynomials are described in equation 3.1. The standard deviation of the measured distances in figure 3.2 is between 0.7 millimeter and 1.7 millimeter and the standard deviation of the measured errors are between 0.6 millimeter and 1.1 millimeter. It is observed that generally the standard deviations of the error is larger when the actual distance is smaller.

$$\begin{aligned} \text{measured distance in millimeters} &= 19.3051\text{nSquares} \\ \text{absolute error in millimeters} &= 0.7193\text{nSquares} \end{aligned} \tag{3.1}$$

3.2 The deformation of the gelatin cuboid

	L_0	ΔL	$\frac{\Delta L}{L_0}$
Top cuboid	3.5 ± 0.2 cm	0.89 ± 0.11 cm	0.25 ± 0.05
Bottom cuboid	3.5 ± 0.2 cm	0.76 ± 0.11 cm	0.22 ± 0.04
Tall cuboid	7 ± 0.2 cm	1.52 ± 0.11 cm	0.22 ± 0.02
Short cuboid	3.5 ± 0.2 cm	0.37 ± 0.11 cm	0.11 ± 0.04

Table 3.1: The deformation of two cubes stacked on top of each other and the deformation of a cuboid twice the size. When two cuboids are stacked on top of each other the deformation of each cuboid is the same. The ratio between the deformation and original length is the same as the cuboid of 7 cm. When the cuboid becomes twice the size the deformation is four times as large.

The position of the phantom relative to the camera is described in figure 2.3, the gelatin phantom is in place of the breast phantom. In table 3.1 the deformation of two stacked cuboids and the deformation of a cuboid twice as high is shown. When two cuboids are stacked on top of each other the deformation of both cuboids is the same, which can not be explained by formula 2.3. The $\frac{\Delta L}{L_0}$ of the stacked cuboids is the same as the $\frac{\Delta L}{L_0}$ of the tall cuboid. The short cuboid has a

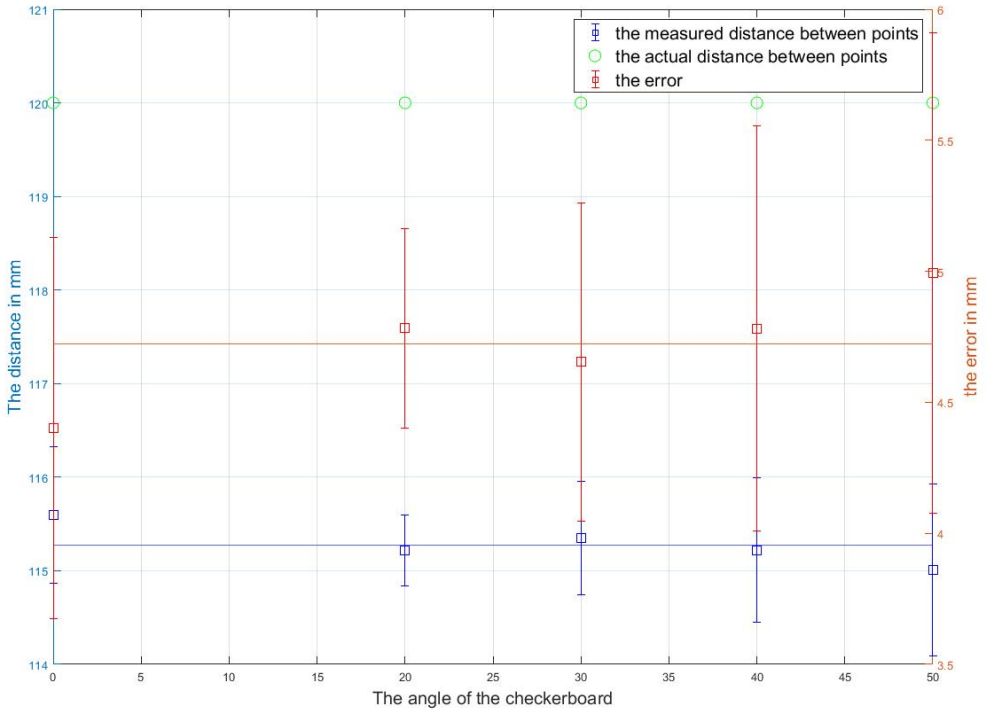

Figure 3.1: The green circles are the actual distance. The red blocks are the measured distances and the standard deviations. The blue blocks are the absolute errors and the standard deviations.

$\frac{\Delta L}{L_0}$ that half the $\frac{\Delta L}{L_0}$ of the tall cuboid. So when the L_0 of the cuboid doubles the ΔL becomes four times as large.

In table 3.2 the deformation of a theoretical cuboid and the deformation of the corresponding FEM model and the deformation of a real cuboid and the deformation of the corresponding FEM model are described. The ΔL of the SOFA cuboid with Youngs modulus 1599 Pa is missing because this simulation was physically unlikely. The difference between the SOFA cuboid with Youngs modulus 2896 Pa and the theoretical cuboid with Youngs modulus 2896 Pa is 0.03 cm, which is an error of 6%, which is exactly the SOFA error of 6%.

3.3 The deformation of the breast phantom

The position of the phantom relative to the camera is described in figure 2.3. In figure 3.3 the Youngs moduli that are tried in SOFA can be found. The height of the phantom before deformation is 9.45 cm. The error has been calculated using 6% of ΔL - the difference between the height before and after deformation. This error is insignificant when the Youngs modulus is larger than 4500 Pa. The height of the actual phantom after deformation is 9.56 $\pm$ 0.11 cm. A Youngs modulus of 4000 Pa caused the same deformation in the SOFA phantom as the real phantom.

The breast phantom before and after deformation with the corresponding FEM overlay are shown in figure 3.4. In table 3.3 can be found the maximum measured error before and after deformation. The difference between these errors is 0.31 cm $\pm$ 0.16. The difference is calculated to take into account the error that existed before deformation.

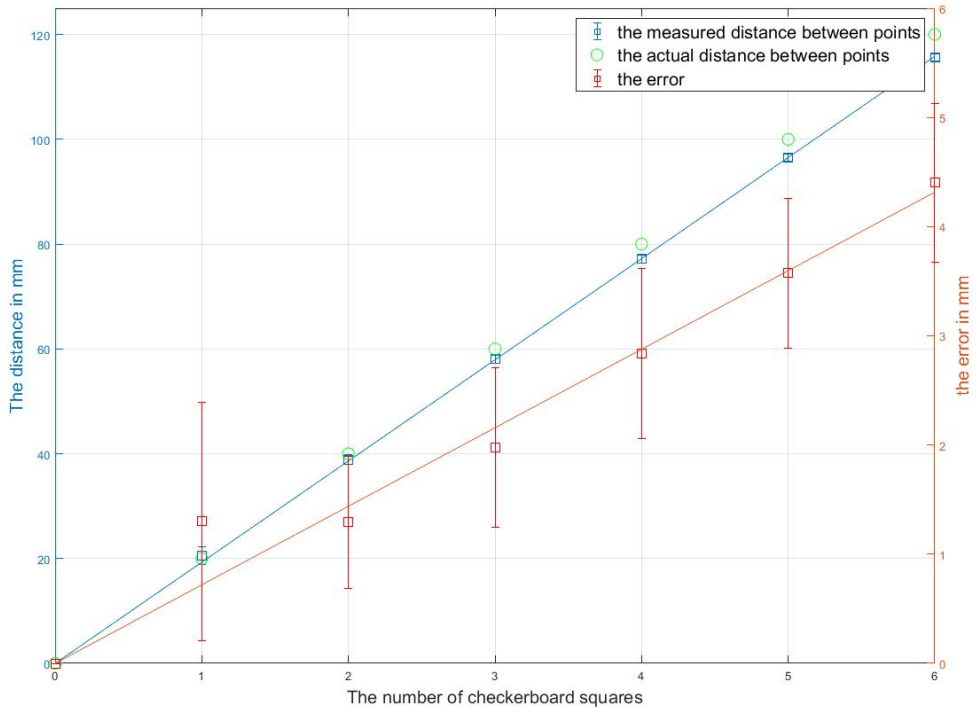

Figure 3.2: The red blocks are the absolute errors per distance and the standard deviations of this error. The blue blocks are the measured distances and the standard deviations. The green dots are the actual distances. The error polynomial is a straight line that crosses the origin with a slope of 0.7193 mm per checkerboard square. This is a systematic error of 4%.

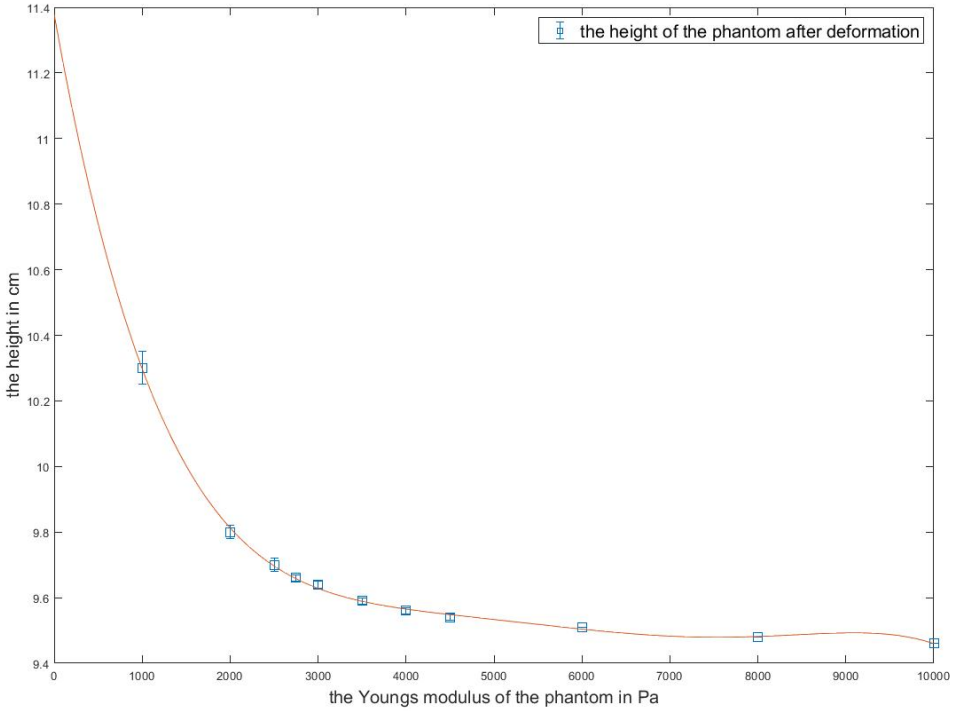

Figure 3.3: The youngs moduli that have been tried in SOFA. The height before deformation is 9.45 cm. The error is calculated using 6% of ΔL - the difference between the height before and after deformation. The error is insignificant for Youngs moduli larger than 4500 Pa. With a Youngs modulus of 4000 Pa the same deformation is achieved as the real phantom. The youngs modulus of 4000 Pa is used for all simulation of the phantom. The height of the actual phantom after deformation is 9.56 $\pm$ 0.11 cm

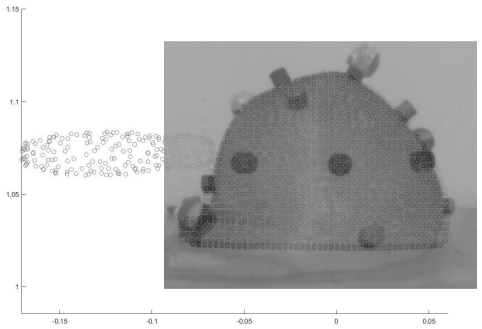

(a) Real phantom with FEM overlay before deformation. A distance of 10 cm is 462 pixels. So one pixel is 0.216 mm.

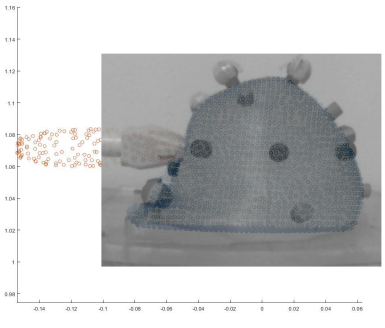

(b) Real phantom with FEM overlay after deformation. A distance of 10 cm is 398 pixels. So one pixel is 0.251 mm.

Figure 3.4: The real phantom with FEM overlay

	L_0 in cm	ΔL in cm	E in Pa
Theoretical cuboid stiff	7.0	0.50	2896
SOFA cuboid stiff 6	7.0	0.47 ± 0.03	2896
Real cuboid soft	7.0	1.5	1599
SOFA cuboid soft	7.0	???	1599

Table 3.2: Comparison between a theoretical cuboid and the corresponding SOFA cuboid and the comparison between a real cuboid and the corresponding SOFA cuboid. The current model is not able to simulate the cuboid with a youngs modulus of 1599 Pa. The current model is able to simulate the cuboid with a youngs modulus of 2896 Pa and the difference between the models is only 0.03 cm. In the state of the art it is described that SOFA has an error of 6% which is exactly 0.03 cm.

	Maximum error in cm
Phantom after deformation	0.83 ± 0.11
Phantom before deformation	0.52 ± 0.11

Table 3.3: The difference between the errors is 0.31 ± 0.16 cm, so the maximum error of the FEM is 0.31 ± 0.16 cm. This is smaller than the value of 0.5 cm that was defined earlier, so the position of the tumor can be predicted accurate enough to do a biopsy of the tumor.

Chapter 4

Discussion

The stereo camera has both a systematic error and random error. The systematic error is likely caused by a calibration error. The random error is likely caused by limitations of the used camera, for example the amount of pixels. The random error is larger when the distance that is measured is smaller.

A possible reason that the numerical model did not correctly predict the deformation of two stacked cubes is because it did not consider the interaction between the two cuboids. When two cuboids are stacked on top of each other they seem to deform as one. To predict the height of both cuboids it has to be calculated at which height the deformed stacked cuboid can be cut in exactly two halves with the same volume. To do this the shape of the cuboid after deformation needs to be predicted.

It is not possible with the current model to simulate soft gelatin. The Youngs modulus of real breast tissue is probably closer to soft gelatin than firm gelatin, so the current model is likely not able to predict the deformation of real breast tissue. In soft materials the Youngs modulus might not be linear, so a non linear Youngs modulus might need to be considered in future research.

To find the Youngs modulus the elongation of the breast phantom while hanging upside down had to be measured. The random error of the stereo camera can cause the height measurement of the phantom to be off by 1.1 mm, so the actual height of the phantom could be between 9.45 cm and 9.67 cm. This means that the actual Youngs modulus could be 2750 Pa and up (the upper limit could not be determined because the corresponding deformations are so small).

The function of the FEM model is to predict the deformation caused by the probe and not to predict the deformation caused by gravity. If the deformation caused by the probe is not influenced much by the Youngs modulus than it might not be needed to simulate the model with the same Youngs modulus as the breast. It might be possible to get sufficient results with a much higher Youngs modulus than the breast.

The current project aims to track deformation of the phantom's body total volume. In this research and previous research only the surface of the breast phantom was tracked, but to evaluate the applicability of the model, the full body must be considered. The phantom is made out of a transparent material so it is possible to add markers in the deeper tissue of the phantom. In future experiments it could be interesting to track markers inside the phantom. The material properties of the phantom causes diffraction of light, so this makes it difficult to use an optical system to track markers inside the phantom, other markers like radioactive markers inside the phantom can also be considered for future research.

Chapter 5

Conclusion

The FEM model is able to predict the deformation of the phantom. When the FEM model of the phantom is simulated with a Youngs modulus of 4000 Pa the deformation caused by gravity is exactly theThe FEM model is able to predict the deformation of the phantom. When the FEM model of the phantom is simulated with a Youngs modulus of 4000 Pa the deformation caused by gravity is exactly the same as the phantom. When the FEM model of the phantom with a Youngs modulus of 4000 Pa is deformed with a probe the largest measured error in is 0.3 cm $\pm$ 0.2, which is smaller than the 0.5 cm that was defined ea

same as the phantom. When the FEM model of the phantom with a Youngs modulus of 4000 Pa is deformed with a probe the largest measured error in is 0.3 cm $\pm$ 0.2, which is smaller than the 0.5 cm that was defined eaned earlier.

To test the FEM model for phantoms with other Youngs moduli the experiment in which deformation is caused by gravity is also conducted on gelatin cuboids. The FEM model accurately predicts the deformation of a gelatin cuboid with a Youngs modulus of 2896 Pa. When the FEM model simulates a cuboid with a Youngs modulus of 1599 Pa it produces physically unlikely results. It is measured that when the cuboid doubles in size the deformation is 4.1 $\pm$ 0.37 times as large, which confirms the prediction of the analytical model. The deformation of two cubes stacked on top of each other can not be explained by the analytical model in equation 2.3, this model predicts a different deformation for each cuboid and in reality both cuboids deform the same amount which can be seen in table 3.1.

The height of the breast phantom and the gelatin phantoms are measured with a stereo camera. The stereo camera has a random error and a systematic error. These errors do not depend on the angle of the checkerboard. The systematic error is 4%, because the stereo camera underestimates the distance with 4%. The random error is 1.1 millimeters.

Bibliography

[1] *RIVM Kans op borstkanker*. URL: https://www.rivm.nl/bevolkingsonderzoek-borstkanker/wat-is-borstkanker/kans-op-borstkanker.

[2] *MURAB MRI and Ultrasound Robotic Assisted Biopsy*. URL: https://www.murabproject.eu/.

[3] Basak Dogan et al. "BI-RADS-MRI: a primer". In: *AJR. American journal of roentgenology* 187 (Sept. 2006), W152–60. DOI: 10.2214/AJR.05.0572.

[4] Vincent Groenhuis et al. "Analytical derivation of elasticity in breast phantoms for deformation tracking". English. In: *International journal of computer assisted radiology and surgery* 13.10 (Oct. 2018). Springer deal, pp. 1641–1650. ISSN: 1861-6410. DOI: 10.1007/s11548-018-1803-x.

[5] Vincent Groenhuis, Francoise J. Siepel, and Stefano Stramigioli. *Real-time Deformation Tracking System for Breast Biopsy*.

[6] Parris Wellman et al. "Breast tissue stiffness in compression is correlated to histological diagnosis". In: *Harvard BioRobotics Laboratory Technical Report* (1999), pp. 1–15.

[7] Babarenda Gamage T, Nielsen P, and Nash M. *Biomechanics of Living Organs: Hyperelastic Constitutive Laws for Finite Element Modeling*. Elsevier Inc, 2017, pp. 215–242.

[8] *Breast - Cancer Staging and Treatment*. URL: https://radiologyassistant.nl/breast/breast-cancer-staging-and-treatment#pathology-ptnm-stage.

[9] Vincent Groenhuis et al. "Analytical derivation of elasticity in breast phantoms for deformation tracking". In: *International journal of computer assisted radiology and surgery* 13.10 (2018), pp. 1641–1650.

[10] Eleonora Tagliabue et al. "Biomechanical modelling of probe to tissue interaction during ultrasound scanning". In: *International Journal of Computer Assisted Radiology and Surgery* (2020).

[11] Vincent Groenhuis et al. "Analytical derivation of elasticity in breast phantoms for deformation tracking". In: *International Journal of Computer Assisted Radiology and Surgery* 13.10 (June 2018), pp. 1641–1650. DOI: 10.1007/s11548-018-1803-x. URL: https://doi.org/10.1007%2Fs11548-018-1803-x.

[12] *MATLAB*. URL: https://nl.mathworks.com/help/matlab/index.html.